

# Effects of base plate wettability on soil-liquid contact angles in sessile drop tests

Mai Sawada

School of Environment and Society, Institute of Science Tokyo, Japan, [sawada.m.af@m.titech.ac.jp](mailto:sawada.m.af@m.titech.ac.jp)

Catherine O'Sullivan

Department of Civil and Environmental Engineering, Imperial College London, the UK

**ABSTRACT:** Soil-liquid contact angles play important roles in soil water retention and suction-induced mechanical properties and are required in particulate numerical modelling of unsaturated soil; however, the reliability of existing methods to measure contact angles is uncertain. We focus on the sessile drop method (SDM) which directly measures the angle between a droplet edge and hydrophilic/hydrophobic soil particles densely arranged on a base plate. The droplet formation was simulated with a two-phase solver in OpenFOAM, an open-source CFD (computational fluid dynamics) code. This simulation approach was used to critically appraise the capacity of the SDM to accurately measure the contact angle by considering the arrangement of particles on the base-plate and both the particle and base-plate wettability. Surface tension was considered by imposing a static contact angle at particle-fluid and base plate-fluid interfaces. The analysis workflow was validated by comparing the simulated and analytical steady-state geometries for a droplet on a flat plate. In the first SDM simulation, particles were regularly arranged on the base-plate and it was seen that the droplet penetrated hydrophilic particles and that the extent to which it spread out on the base plate increased as the base plate-fluid contact angle reduced. The measured contact angle decreased with increasing base plate wettability and mostly differed from the particle-fluid contact angle specified in the simulation. Experimental studies typically ignore the effects of base plate wettability in SDM tests. However, the data presented here indicate that the SDM cannot provide accurate soil-fluid contact angles for hydrophilic particles if the droplet penetrates the particle layer and touches the base-plate.

**KEYWORDS:** Unsaturated soil, CFD analysis, granular soil.

## 1 INTRODUCTION

Water is retained in unsaturated granular soil due to surface tension at the air-water interface in pores with implications for hydraulic conductivity and material strength. The amount of water retained in the soil increases with decreasing orientation of the soil particle-water interface ( $\theta$ ) as the vertical component of capillary force increases. Jurin's law theoretically predicts the contact angle effects on the capillary height in a straight tube; however, the bundle of capillary tubes model (Blunt, 2017), which adopts Jurin's law, often assumes  $\theta = 0^\circ$  for simplicity. Sawada et al. (2025) numerically simulated hysteretic drying and wetting processes in single-pore and sphere packing models and showed that the observed water retention curves were sensitive to  $\theta$ . The suction at the water entry into pores during the wetting process is particularly sensitive to  $\theta$ . Consequently,  $\theta$  also impacts the suction-induced stiffness and strength as well as hydraulic conductivity. In simulations of unsaturated materials using the discrete element method (DEM),  $\theta$  is a key parameter in the contact model adopted and impacts the predicted inter-particle forces (e.g. Lu and Lechman, 2008).

While the importance of  $\theta$  is well-established, the reliability of existing experimental methods to measure  $\theta$  is uncertain. Three methods; the capillary rise method (CRM), the sessile drop method (SDM) and the water drop penetration test (WDPT) are commonly used for granular soil. In the CRM which uses Washburn's equation,  $\theta$  is indirectly determined by measuring the capillary height in the hydrophilic (i.e.  $\theta < 90^\circ$ ) sample packed in a tube. Siebold et al. (1997) improved measurement accuracy by measuring the sample weight change instead of relying on visual observation of the capillary height. Liu et al. (2014) proposed a further modified method; however, the measured  $\theta$  showed unexpected particle size dependency. In the SDM test which is used for both hydrophilic and hydrophobic materials,  $\theta$  is directly obtained by measuring the angle between a droplet edge and a sample of particles arranged on a flat base-plate. Bachmann et al. (2000a) applied the SDM to soil particles arranged on an adhesive tape attached to a base plate; however, the measured  $\theta$  had large variations,

particularly for hydrophilic samples. The WDPT is used to distinguish hydrophilic and hydrophobic materials from the penetration time of a droplet on a soil bed, but it does not provide exact  $\theta$  values (Bachmann et al., 2000b).

This study focuses on the SDM and examines the factors which impact the test results. The droplet formation was simulated with a two-phase solver in OpenFOAM, an open-source CFD (computational fluid dynamics) code. The simulation has enabled the identification of key factors that determine measurement accuracy as the impact of particle arrangement and wettability could be considered in detail. We considered droplet formation on hydrophilic particles arranged on a base plate and examined the impacts of the base plate wettability on the measured  $\theta$  of granular soil.

## 2 MODEL DEVELOPMENT

The simulation used the finite-volume method, specifically interFoam, a two-phase incompressible transient solver in OpenFOAM v2012 (Open CFD, 2020). Standard fluid properties shown in Table 1 were used as per the user guide for OpenFOAM (OpenFOAM Foundation, 2020), and laminar flow was assumed. The fluid-fluid interface is captured with the volume of fluid (VOF) method, in which an indicator function  $\alpha$  ( $0 \leq \alpha \leq 1$ ), represents the volume fraction of fluid in each cell. In the model,  $\alpha = 1$  when a cell is filled with water and  $\alpha = 0$  when a cell is filled with air, an air cell has  $0 \leq \alpha \leq 0.5$ , and a water cell has  $0.5 \leq \alpha \leq 1$ .

Table 1. Fluid properties.

Property	Water	Air	Air-water interface
Fluid type	Newtonian	Newtonian	-
Kinematic viscosity (m <sup>2</sup> /s)	$1 \times 10^{-6}$	$1.48 \times 10^{-5}$	-
Density (kg/m <sup>3</sup> )	1000	1	-
Surface tension (N/m)	-	-	0.0707106

Figure 1 shows numerical models for simulating the droplet test. A strip model with periodic conditions on the front

and back sides was employed as its computational cost was smaller than that of an axially-symmetric hemisphere model although the two models provided similar results. Symmetric conditions were used for the right and left boundaries. Surface tension was considered by imposing a static contact angle at the sphere-fluid ( $\theta_s$ ) and base plate-fluid ( $\theta_p$ ) interfaces. The velocity was fixed at 0 m/s, and the pressure gradient was set to achieve zero flux on the sphere-/plate-fluid interfaces. The gradient in  $\alpha$  at the top boundary (exposed to the atmosphere) was fixed at zero. The velocity gradient was fixed at zero for outflow and the inflow velocity was obtained from the flux with the inlet direction.

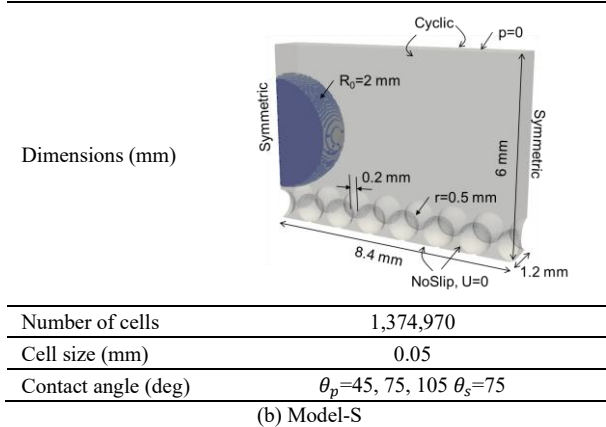
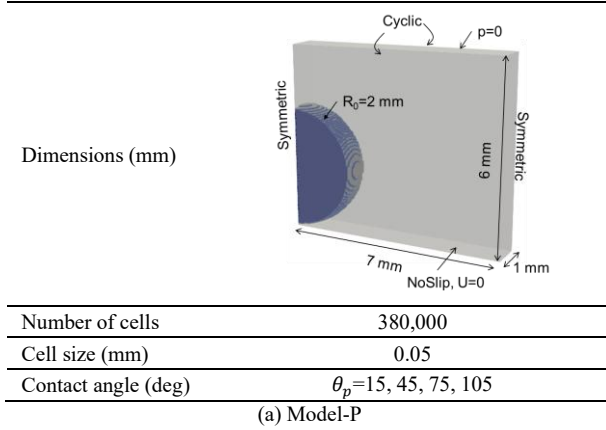


Figure 1. Numerical models.

Model-P (Figure 1 (a)) was developed to validate the simulation workflow, while Model-S (Figure 1 (b)) was designed to simulate the SDM test. Model-P simply considered a flat plate, while in Model-S spheres with a radius of 0.5 mm were arranged on a base plate with an inter-particle distance of 0.2 mm. In both the Model-P and the Model-S simulations, a droplet was initially set above the plate in Model-P / the spheres in Model-S, and the droplet deformation due to surface tension was recorded until the deformation ceased, after about 0.2 s from the start. Gravity was not considered in both the Model-P and the Model-S simulations. The cell size selected was 0.05 mm, i.e. there were 20 cells per particle diameter. The resolution was determined based on the granular packing models used for capillary rise simulations in Sawada et al. (2025). The timestep was automatically controlled to keep each CFD cell's Courant number under 1 and it varied between  $1 \times 10^{-7}$  and  $1 \times 10^{-6}$  s.

The droplet size was determined by considering laboratory tests. While the SDM method is less frequently applied to sand in comparison to silt and clay; Bachman et al. (2000a), Bachman et al. (2003) and Ramírez-Flores et al., (2010), give

some guidance on the appropriate drop size for a given particle size. They used 10  $\mu\text{l}$  drops for sand ( $d < 630 \mu\text{m}$ ), corresponding to 77 times the sand grain volume. Aligned with these experiments, the simulation drop volume was set at 33.5  $\mu\text{l}$  ( $R_0=2$  mm), which corresponds to 64 times the particle volume ( $d=1$  mm).

### 3 DROPLET SIMULATION

#### 3.1 Model validation

Model-P was used to validate the simulation work-flow. In the absence of gravity, the steady-state droplet height ( $e$ ) and length ( $L$ ) for a droplet on a flat plate can be analytically obtained assuming a circular cap droplet (Dupont & Legendre 2010):

$$e = R(1 - \cos \theta_p) \quad (1)$$

$$L = R \sin \theta \quad (2)$$

$$R = \sqrt{\frac{\pi \left( 2R_0^2 + \frac{2}{3}d^2 \right)}{\theta_p - \sin \theta_p \cos \theta_p}} \quad (3)$$

where  $R_0$  is the initial droplet radius (i.e., 2 mm),  $R$  is the steady-state radius of curvature, and  $d$  is the half depth of the domain (i.e., 0.5 mm).

Figure 2 compares the simulated and analytical steady-state  $e$  and  $L$  values normalised by  $R$  for  $\theta_p=15^\circ, 45^\circ, 75^\circ$  and  $105^\circ$ . The simulated values matched the analytical solutions; however, the discrepancy was relatively large when  $\theta_p=15^\circ$  because the droplet continued to deform (at a slow rate) even after 1.2 s.

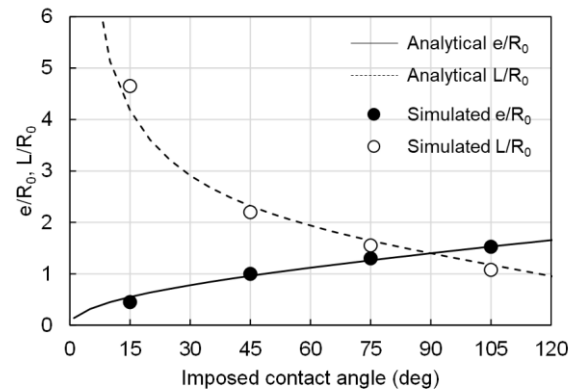


Figure 2. Model validation.

In the SDM,  $e$  and  $L$  are commonly measured with optical methods and the contact angle at the surface-fluid interface ( $\theta_{meas}$ ) is obtained with a schematic method called the half angle method (HAM) that assumes a circular cap when the gravity effects are negligible (Gu et al., 2016):

$$\tan \frac{\theta_{meas}}{2} = \frac{2e}{L} \quad (4)$$

$\theta_{meas}$  from the simulated  $e$  and  $L$  matched the contact angles locally measured from the coordinates of points in the vicinity of the droplet edge. These data show that the HAM can provide reasonable  $\theta_{meas}$  on both a planar and sphere surface in the absence of gravity.

#### 3.2 Effects of base-plate wettability

In the Model-S simulation, the droplet penetrated through the hydrophilic spheres and touched the base-plate. Similar results

were obtained even when the spheres were densely arranged and contacted each other. Figure 3 shows the droplet formation process in Model-S when  $\theta_{s\_imposed}=75^\circ$  and  $\theta_p=45^\circ$ . The droplet placed on the center sphere penetrated the pores due to downward surface tension acting on the wetting front, and then touched the base-plate and spread.

Figure 4 shows the changes in the droplet top height and the length from the left side boundary to droplet edge in the early stage up to 0.1 s when  $\theta_p=45^\circ$ ,  $75^\circ$  and  $105^\circ$ , and  $\theta_{s\_imposed}=75^\circ$ . Figure 5 shows the steady-state droplets at 0.2s with the three different  $\theta_p$  values. In Model-S,  $\theta_{s\_meas}$  was obtained via the HAM by measuring the droplet height from the elevation where the droplet edge perched on the sphere (i.e., slightly lower than 1 mm from the base plate) and the droplet length at the droplet edge elevation.

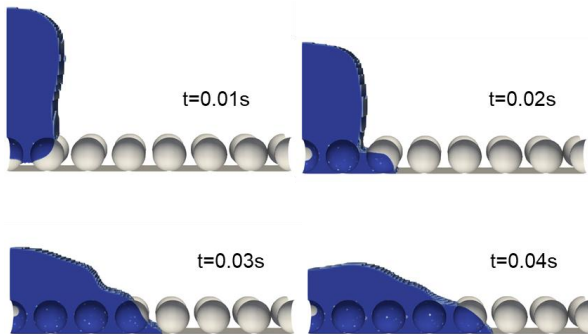


Figure 3. Droplet formation ( $\theta_{s\_imposed}=75^\circ$  and  $\theta_p=45^\circ$ ).

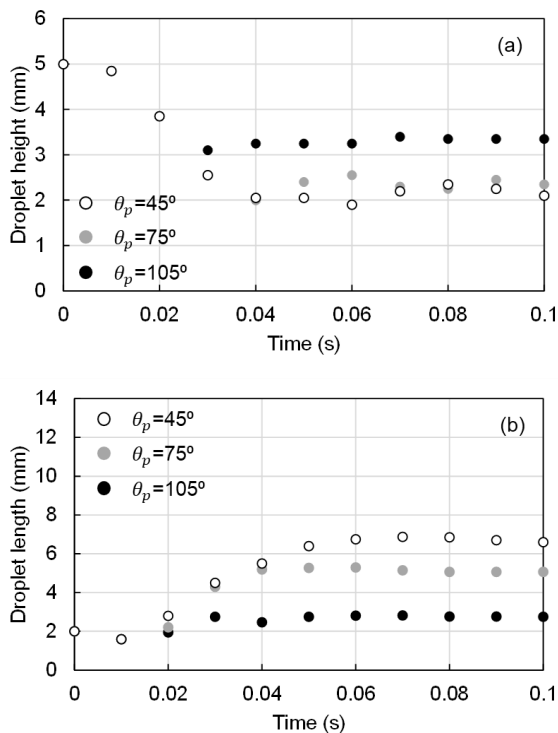


Figure 4. Droplet geometry change: (a) height and (b) length.

Figure 6 considers steady-state  $\theta_{s\_meas}$  values as a function of the base plate contact angle for  $\theta_{s\_imposed}$  of  $75^\circ$ . The results show that in two of the three simulations  $\theta_p \neq \theta_{s\_imposed}$ , the base plate wettability greatly impacted the droplet geometry and  $\theta_{s\_meas}$  increased with increasing  $\theta_p$ . This indicates that the SDM does not provide accurate soil-fluid contact angles

when the droplet touches the base plate and provides additional insights to experimental studies which ignore the base plate effects. Bachmann et al. (2000b) discussed the effects of adhesive tape ( $\theta_p \sim 90^\circ$ ) on the base plate from experiments on samples with different ratios of hydrophobic treated particle. They indirectly concluded that the adhesive tape effects were limited just because the  $\theta_{s\_meas}$  sensitively reacted to the treated particle ratio; however, the effects did not directly examined. The simulation results suggest that the adhesive tape can contribute to the variation in  $\theta_{s\_meas}$  and the discrepancy from the actual particle-fluid contact angle. The test results were less sensitive to the base plate wettability when soil particles were densely arranged to reduce the base plate area; however, they cannot be removed as long as the droplet touches the base plate.

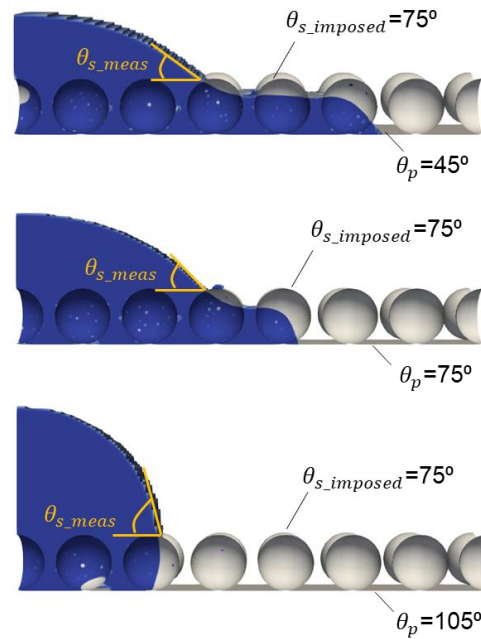


Figure 5. Steady-state droplets with different base plate wettability.

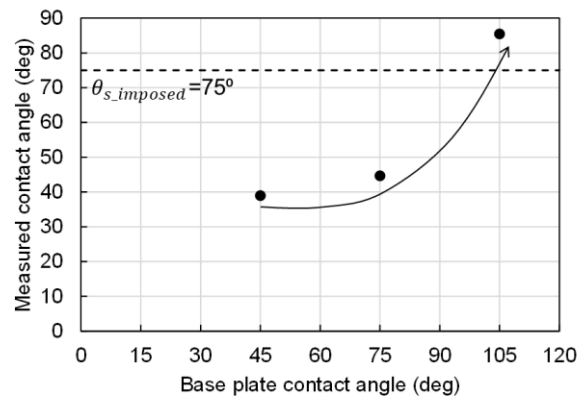


Figure 6. Effects of  $\theta_p$  on  $\theta_{s\_meas}$ .

#### 4 CONCLUSIONS

This study used sub-particle-scale computational fluid dynamics (CFD) simulations to explore the effects of base-plate wettability on the granular soil-fluid contact angle measured in SDM tests used to quantify soil-water contact angle. The simulation results showed that the measured soil particle-fluid

contact angles significantly increased with decreasing base plate wettability. The measured contact angles mostly differed from the real contact angles input to the simulation model when the droplet penetrated the sample particles and touched the base plate. These data indicate that SDM cannot be used for hydrophilic samples where the droplet penetrates and the base plate wettability affects the droplet formation.

## 5 ACKNOWLEDGEMENTS

All OpenFOAM simulations were performed on the Imperial College London Research Computing System facilities (DOI: 10.14469/hpc/2232). Funding from the Canon Foundation in Europe also supported this study.

## 6 REFERENCES

- Bachmann, J., Ellies, A. and Hartge, K. H. 2000a. Development and application of a new sessile drop contact angle method to assess soil water repellency. *Journal of Hydrology* 231, 66-75.
- Bachmann, J., Horton, R., Van Der Ploeg, R. R. and Woche, S. 2000b. Modified sessile drop method for assessing initial soil–water contact angle of sandy soil. *Soil Science Society of America Journal* 64(2), 564-567.
- Bachmann, J., Woche, S. K., Goebel, M. O., Kirkham, M. B. and Horton, R. 2003. Extended methodology for determining wetting properties of porous media. *Water resources research* 39(12).
- Blunt, M. J. 2017. *Multiphase flow in permeable media: A pore-scale perspective*. Cambridge, UK: Cambridge University Press.
- Dupont, J. B. and Legendre, D. 2010. Numerical simulation of static and sliding drop with contact angle hysteresis. *Journal of Computational Physics* 229(7), 2453-2478.
- Gu, H., Wang, C., Gong, S., Mei, Y., Li, H. and Ma, W. 2016. Investigation on contact angle measurement methods and wettability transition of porous surfaces. *Surface and Coatings Technology* 292, 72-77.
- Lechman, J. and Lu, N. 2008. Capillary force and water retention between two uneven-sized particles. *Journal of Engineering Mechanics* 134(5), 374-384.
- Liu, Z., Yu, X. and Wan, L. 2016. Capillary rise method for the measurement of the contact angle of soils. *Acta Geotechnica* 11, 21-35.
- Open CFD. 2020. Open CFD Release OpenFOAM® v2012. [Online] Available at: <https://www.openfoam.com/news/main-news/openfoam-v20-12>. [Accessed 9<sup>th</sup> December, 2023].
- OpenFOAM Foundation. 2020. OpenFOAM v8. [Online] Available at: <https://doc.cfd.direct/openfoam/user-guide-v8/>. [Accessed 9<sup>th</sup> December, 2023].
- Ramírez-Flores, J. C., Bachmann, J. and Marmur, A. 2010. Direct determination of contact angles of model soils in comparison with wettability characterization by capillary rise. *Journal of Hydrology* 382(1-4), 10-19.
- Sawada, M., O’Sullivan, C., Tsiamposi, A and Salomon, J. 2025. Insight into hysteretic drying and wetting in unsaturated granular soil from fully resolved computational fluid dynamics analysis. *Journal of Engineering Mechanics* 151(6), 04025018.
- Siebold, A., Walliser, A., Nardin, M., Oppliger, M. and Schultz, J. 1997. Capillary rise for thermodynamic characterization of solid particle surface. *Journal of colloid and interface science* 186(1), 60-70.